frontiers | Frontiers in Earth Science

TYPE Original Research
PUBLISHED 23 June 2023
DOI 10.3389/feart.2023.1212017

OPEN ACCESS

EDITED BY
Lijie Guo,
Beijing Mining and Metallurgy Technology Group Co. Ltd., China

REVIEWED BY
Xinglan Cui,
General Research Institute for Nonferrous Metals, China
Zhihong Zhang,
Beijing University of Technology, China

*CORRESPONDENCE
Zhongqun Guo,
guozhongqun_jxust@163.com

RECEIVED 25 April 2023
ACCEPTED 12 June 2023
PUBLISHED 23 June 2023

CITATION
Guo Z, Liu L, Zhou K, Wang X and Zhong W (2023), Research on the saturated/unsaturated seepage laws of ionic rare earth ore under different leaching conditions.
Front. Earth Sci. 11:1212017.
doi: 10.3389/feart.2023.1212017

Research on the saturated/unsaturated seepage laws of ionic rare earth ore under different leaching conditions

Zhongqun Guo[1,2]*, Lingfeng Liu[1], Kefan Zhou[1], Xiaojun Wang[2] and Wen Zhong[2]

[1]School of Civil Engineering and Surveying and Mapping Engineering, Jiangxi University of Science and Technology, Ganzhou, China, [2]Jiangxi Key Laboratory of Mining Engineering, Jiangxi University of Science and Technology, Ganzhou, China

The seepage law of the ionic rare earth leaching process plays an important role in the efficient development and utilization. The saturation permeation test of ionic rare earth under different leaching conditions was carried out using the variable head method, and the influence of type, concentration, and leaching path on the saturation permeability coefficient was revealed. The relationship between the water content and the matric suction of ionic rare earths under different leaching conditions was measured with the Geo-Experts pressure plate apparatus, and the soil-water characteristic curves under different leaching conditions were obtained. Based on the soil-water characteristic curve model, the unsaturated permeability coefficient function of ionic rare earths under different conditions was studied. The results show that the saturated-unsaturated permeability coefficients of ionic rare earths are pure water, 3% $(NH_4)_2SO_4$, and 3% $MgSO_4$, in descending order, when the type of leaching solution is different. For different concentrations of the leaching solution, when the concentration of $(NH_4)_2SO_4$ increases from 2% to 5%, the saturated permeability coefficient first increases and then decreases. The matrix suction is an important factor affecting the unsaturated permeability coefficient when the ore body is unsaturated, and the unsaturated permeability coefficient decreases with the increase of the leaching solution concentration under the same matric suction. The seepage law is related to the leaching path, and the permeability coefficient increases when leaching at high concentrations followed by low concentrations, in reverse order, the permeability coefficient decreases. The research results can provide theoretical guidance for the design of injection parameters, and improve the theory of in-situ leaching.

KEYWORDS

ionic rare earths, in-situ leaching, soil-water characteristic curve, saturated permeability coefficient, unsaturated permeability

1 Introduction

Ionic rare earths are an important strategic mineral resource and play an important role in the national defense industry and high-precision technology products (Ilankoon et al., 2018; Nie et al., 2020; Liu et al., 2021). In these ores, rare earth elements, which are adsorbed on the clay minerals through hydrated cations or hydroxyl-hydrated cations, are difficult to enrich by conventional selection techniques. After years of research by scientific and technological workers, ionic rare earths have successively experienced the mining methods of pool leaching, heap

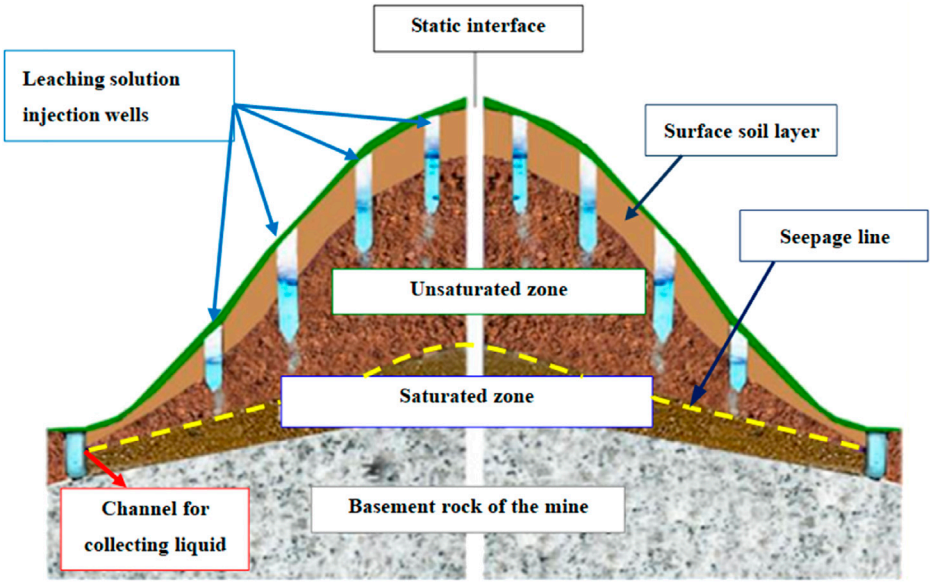

FIGURE 1
Diagram of ionic rare earth *in situ* leaching.

leaching, and *in-situ* leaching (Zhang et al., 2016; Chi et al., 2019; Zhou et al., 2019). *In-situ* leaching has the advantages of being a simple process with low cost and low disruption, and is currently widely recommended (Deng et al., 2016; He et al., 2017). The schematic diagram of *in situ* leaching is shown in Figure 1. The permeability of the ore body has an important impact on the *in situ* leaching velocity and leaching rate, which are directly related to the efficient recovery and utilization of rare earth resources. The seepage of *in situ* leaching is a dynamic process that includes two stages: unsaturated and saturated seepage. It is of great significance to study the saturated-unsaturated permeation characteristics of ionic rare earths under different leaching conditions to improve leaching efficiency.

During the *in situ* leaching process, parameters such as water content, matric suction, and permeability coefficient all changed (Wu et al., 2005; Long et al., 2019). Many scholars have conducted relevant studies on the saturation permeation characteristics of ionic rare earths. (Yin et al., 2015; Yin et al., 2018) studied the relationship between particle size and capillary rise rate, pore ratio, and permeability of ionic rare earth ore. (Jin et al., 2015; Guo et al., 2017) investigated the influence of particle size of ionic rare earth ore on the one-dimensional vertical seepage law. (Guo et al., 2020) wrote about the effects of particle size and grain composition on the two-dimensional infiltration characteristics of ionic rare earths. (Wang et al., 2017) studied the seepage mechanism of ionic rare earths at the microscopic and mesoscopic scales. Currently, the research on the seepage characteristics of ionic rare earth ore mainly focuses on saturated permeation, and the research on unsaturated permeability characteristics is inadequate. Since the unsaturated permeability coefficient is difficult to be directly measured by experiments, the soil-water characteristic curve model and the saturated permeability coefficient are typically used to derive the unsaturated permeability coefficient function and reveal the unsaturated permeability law of rock and soil (Ma et al., 2016).

In this study, rare earth ore samples from Jiangxi Province were selected to carry out saturation seepage experiments and soil-water characteristic experiments; the saturated permeability coefficient and soil-water characteristic curve of the ore body under different leaching conditions were obtained and revealed the saturated/unsaturated seepage law of ionic rare earths under different types, concentrations, and leaching paths, which provided a theoretical basis for the prediction of the *in situ* leaching rate and the regulation of the leaching solution injection.

2 Test materials and methods

2.1 Test materials

The ore samples were selected from a rare earth mine in Longnan, Jiangxi Province. The basic physical parameters of the samples are listed in Table 1. The particle size distribution curve of rare earth ore is shown in Figure 2.

The samples were remolded in accordance with the dry density and water content of the undisturbed soil. The quantitative X-ray diffraction (XRD) analysis of the ore samples was carried out, and the results are shown in Figure 3.

2.2 Test devices and methods

The saturation permeability coefficient was measured using the TST-55 variable head permeameter (Gao et al., 2008). The device is shown in Figure 4. The samples were saturated with a vacuum saturator for 24 h, and then the saturation penetration experiment was carried out to measure the saturation

TABLE 1 Basic physical parameters of rare earth ores.

Density ρ/ (g·cm^{-3})	Water content θ/%	Specific gravity G_s/ (g·cm^{-3})	Void ratio e	Liquid limit w_L/%	Plastic limit w_P/%	Plastic index I_p
1.43	16.46	2.68	0.86	41.17	30.83	10.34

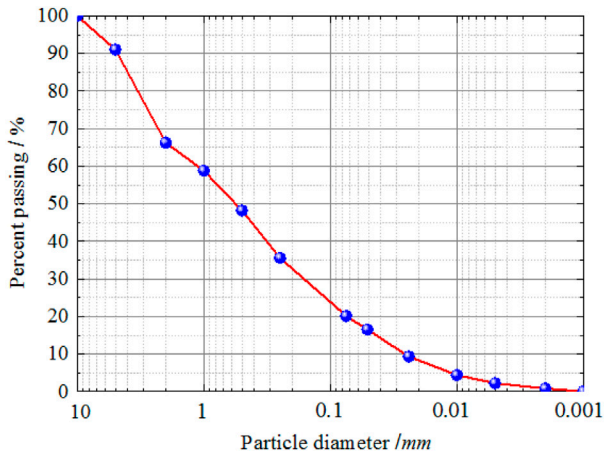

FIGURE 2
Particle size distribution curve of rare earth ore sample.

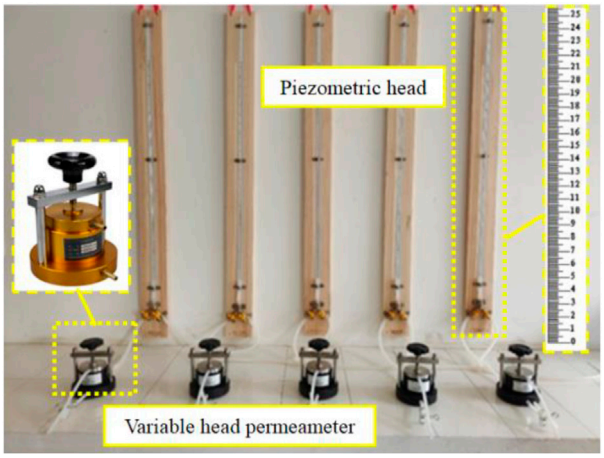

FIGURE 4
The saturation penetration apparatus.

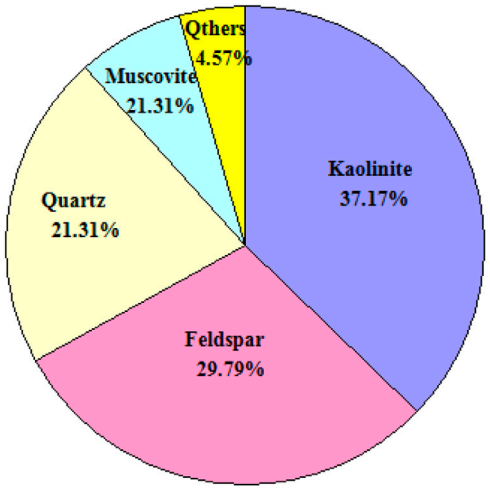

FIGURE 3
XRD mineral composition analysis of rare earth ore samples.

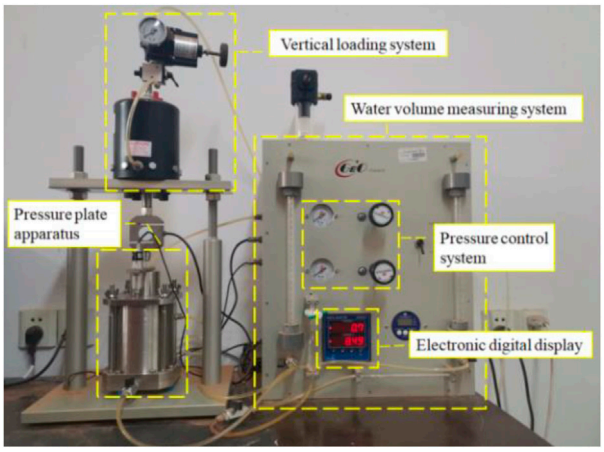

FIGURE 5
The Geo-Experts pressure plate test apparatus.

permeability coefficient of ionic rare earth under different types, concentrations, and leaching paths.

The Geo-Experts pressure plate apparatus was used for the soil-water characteristic experiment, and the device is shown in Figure 5. First, ionic rare earth samples were prepared and saturated with leaching solution under the same conditions, and then the soil-water characteristic experiments were carried out to measure the corresponding soil-water content under different matrices of suction. For a single matrix suction, when the 24 h change was less than 0.1 mm, the equilibrium state was considered to have been reached under that specific matric suction (Pham et al., 2005; Fredlund et al., 2006).

2.3 Data calculation

The following logarithmic formula was used to calculate the saturated permeability coefficient of ionic rare earths:

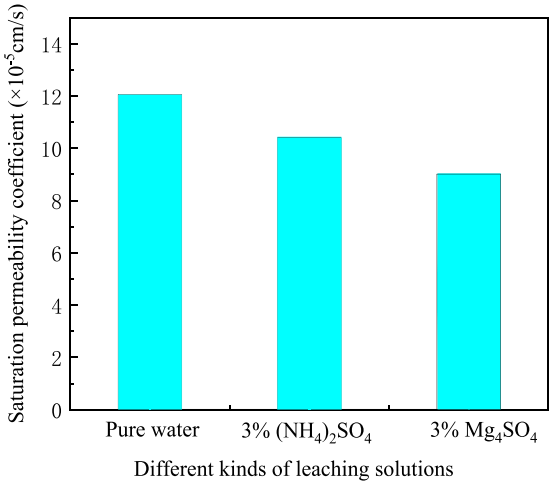

FIGURE 6
Saturated permeability coefficients for different leaching solutions.

$$k_T = 2.3\frac{aL}{A\Delta t}\ln\frac{h_1}{h_2} \quad (1)$$

where k_T is the saturation permeability coefficient; a is the cross-sectional area of the variable head pipe; A is the cross-sectional area of the cutting ring; the value of 2.3 is the conversion factor of ln; L is the height of the cutting ring; Δt is the start and end interval of the measured water head; h_1 and h_2 are the start and end water heads.

For the soil-water characteristic curve of ionic rare earths, the mass water content under different matric suction was measured experimentally and converted into volume water content, and the matric suction and volume water content at all levels were plotted in a semi-logarithmic coordinate system to obtain the corresponding soil-water characteristic curve. The corresponding volume water content of the different matrices suction is:

$$\theta = \frac{w\rho_d}{\rho_w} \quad (2)$$

where θ is the volume water content, w is the mass water content, ρ_d is the dry density of soil, and ρ_w is the density of water.

The soil-water characteristic curve is the basis for research on the permeability characteristics of unsaturated soil, and many scholars have proposed the relevant soil-water characteristic curve model (Van Genuchten et al., 1980; Rajkai et al., 1996; Chiu et al., 2012). Research shows that the Fredlund and Xing model has high adaptability to the soil-water characteristic curve of ionic rare earths (Guo et al., 2021); therefore, their three-parameter model was used for analysis. The expression of Fredlund and Xing's three-parameter model (Fredlund et al., 1994) is as follows:

$$\frac{\theta}{\theta_s} = \frac{1}{\left\{\ln\left[e + \left(\frac{\psi}{a}\right)^n\right]\right\}^m} \quad (3)$$

where θ is the volume water content, θ_s is the saturated water content, and ψ is the matrix suction. a, n, and m are the three optimization parameters of the model. The parameter a is related to the air-entry value, n is a parameter related to the drying rate and it controls the slope of the SWCC, m is a parameter related to the residual water and it is correlated with the overall symmetry of the curve. This model assumes that there is a small θ_r. For simplification of the models, it is hypothesized that θ_r=0.

3 Saturation seepage law for ionic rare earths under different leaching conditions

3.1 Saturation permeability under different leaching solutions

The saturated permeability coefficients of ionic rare earth under the different types of leaching solutions are shown in Figure 6. When the leaching solution was pure water, 3% $(NH_4)_2SO_4$, and 3% $MgSO_4$, the corresponding saturation permeability coefficients were 12.05 × 10^{-5} cm/s, 10.4 × 10^{-5} cm/s, and 9.01 × 10^{-5} cm/s, respectively. It can be seen that the saturation permeability coefficient decreased sequentially. The analysis suggests that in the seepage process, pure water did not undergo a chemical exchange reaction with rare earth ions, the migration and agglomeration of soil particles resulted in an increase of the effective seepage channel in the soil, and then the saturated permeability coefficient of pure water was greater.

When the leaching solution was 3% $MgSO_4$ and 3% $(NH_4)_2SO_4$, both underwent chemical exchange reactions with rare earth ions adsorbed on clay minerals. The exchange reactions between NH^{4+}, Mg^{2+} and rare earth ions cause the agglomeration, disintegration, and migration of soil particles, resulting in the blockage of seepage channels; therefore, the permeability characteristic was reduced. Consequently, the saturated permeability coefficients of 3% $(NH_4)_2SO_4$ and 3% $MgSO_4$ were significantly smaller than those of pure water. The chemical exchange reaction formula is as follows:

$$\left[Al_2Si_2O_5(OH)_4\right]_m \cdot 2nRE^{3+}(s) + 3nMg^{2+}(aq) \rightleftharpoons \left[Al_2Si_2O_5(OH)_4\right]_m \cdot \left[Mg^{2+}\right]_{3n}(s) + 2nRE^{3+}(aq)$$

$$\left[Al_2Si_2O_5(OH)_4\right]_m \cdot 2nRE^{3+}(s) + 3nNH_4^+(aq) \rightleftharpoons \left[Al_2Si_2O_5(OH)_4\right]_m \cdot \left[NH_4^+\right]_{3n}(s) + nRE^{3+}(aq)$$

The results show that the cations adsorbed on the clay can exchange with the divalent cation in the solution during the permeation experiment, thereby resisting the dispersion of soil particles and preventing the formation of micro-fissures. Similar results were obtained with Mg^{2+} in this experiment. For the leaching solution of 3% $MgSO_4$, Mg^{2+} not only reacted with the divalent cations adsorbed by clay minerals but also exchanged reactions with the monovalent cation therein, adsorbed on the surface of ionic rare earth particles, so that the thickness of the combined water layer increased, at the same time leading to the reduction of the porous channel between the particles, further reducing the permeability characteristic of ionic rare earth. Consequently, the permeability coefficient of 3% $MgSO_4$ appeared to be slightly lower than that of 3% $(NH_4)_2SO_4$.

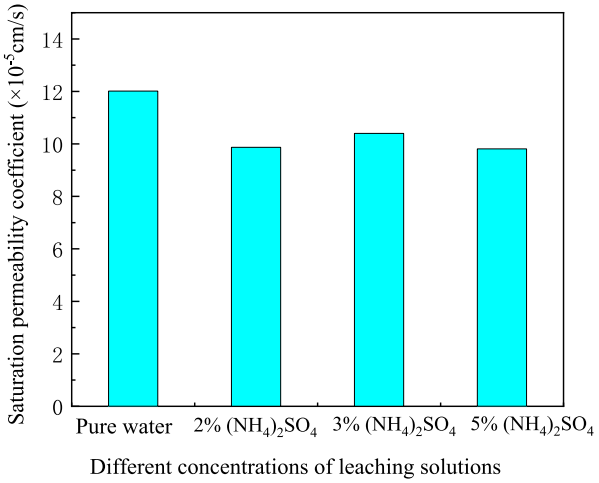

FIGURE 7
Saturated permeability coefficient under different concentrations of leaching solution.

3.2 Saturation permeability at different leaching solution concentrations

The saturated permeability coefficients of ionic rare earth under different concentrations of leaching solution are shown in Figure 7, and the saturated permeability coefficients of ionic rare earth corresponding to pure water, 2% $(NH_4)_2SO_4$, 3% $(NH_4)_2SO_4$, and 5% $(NH_4)_2SO_4$ are 12.05× 10^{-5} cm/s, 9.87 × 10^{-5} cm/s, 10.4 × 10^{-5} cm/s, and 9.81 × 10^{-5} cm/s, respectively. It can be seen that the saturation permeability coefficient is the largest under the leaching of pure water, and when the concentration of the leaching solution increased from 2% to 5%, the saturation permeability coefficient increased and then decreased, with the saturation permeability coefficient under the leaching of 3% $(NH_4)_2SO_4$ being greater than in the other two conditions.

It is believed that the concentrations of leaching solution have a certain influence on the structure of the electrical double layer of the soil. The double layer on the surface of the soil particles includes an adsorption layer and a diffusion layer, and during the seepage process, the diffusion layer moved with the cations. The thickness of the electrical double layer is closely related to the ion concentration, and with the increase in concentration of the leaching solution, the diffusion layer will decrease, so the seepage channel will expand, and the permeability coefficient will increase.

In the seepage process, NH^{4+} and the rare earth ions on the surface of the clay mineral underwent chemical exchange reactions, and the more NH^{4+} of leaching solution, the smaller saturation permeability coefficient appears. At the same time, the electrical double layer on the surface of the soil particles was affected, but the effect of the ion exchange reaction was less than the weakening effect of the thickness of the double electrical layer.

With the increase of concentration, the ion exchange reaction became more violent , and the weakening effect of the electric double layer began to be lower than that of the ion exchange reaction, thereby inhibiting the seepage effect, making the permeation characteristics smaller. Considering the combined influence of the double electrical layer and the ion exchange reaction degree, the saturation permeability coefficient of the ore body under the leaching of 5% $(NH_4)_2SO_4$ was found to be smaller than that of 3% $(NH_4)_2SO_4$.

3.3 Saturation permeability under different leaching paths

The leaching solution was set as $(NH_4)_2SO_4$, and two groups of experiments were set up for control: "first high concentration followed by low concentration" and "first low concentration followed by high concentration," respectively. "First high concentration followed by low concentration" means that ionic rare earths used a high concentration leaching solution for saturated leaching for 24 h before the seepage experiment, and then used a low concentration leaching solution for seepage. Three working conditions were set: 3%→3%, 3%→1%, 3%→0%. In contrast, a low concentration leaching solution was used for saturation solution for 24 h, and then a high concentration leaching solution was used to seep, with three working conditions being set: 0%→3%, 1%→3%, 3%→3%. The relationship between the saturated permeability coefficient of the ore body under different leaching paths is shown in Figure 8.

It can be seen from Figure 8A that the saturated permeability coefficient of ionic rare earths under the leaching of 3%→3%, 3%→1%, 3%→0% was 10.40 × 10^{-5} cm/s, 10.67 × 10^{-5} cm/s, and 8.42 × 10^{-5} cm/s, respectively. The saturation permeability coefficient of the ore body showed little difference. The saturated permeability coefficient under the leaching of 3%→1% increased slightly, and the leaching of 3%→0% was the smallest.

Our analysis shows that during the "first high concentration followed by low concentration" phase, as the free water diffused from a high concentration to a low concentration, the soil particles produced a repulsive force from the inside to the outside, causing the soil particles to break, blocking the seepage channel, and reducing permeability. At the same time, the ion exchange reaction was weakened, the effect on soil particles was reduced, and the permeability of ionic rare earths improved. Under 3%→0% working conditions, the permeability was reduced by the larger concentration difference. At this time, the effect of the ion exchange reaction was less than that of the seepage; therefore, its saturation permeability coefficient was minimal. Under 3% →1% working conditions, the difference in concentration was smaller than that of 3%→0% working conditions, the repulsive force was also smaller, and the degree of permeability was relatively small.

It can be seen from Figure 8B that the saturated permeability coefficient of ionic rare earth under the leaching of 3%→3%, 1%→3%, 0%→3% was 10.40 × 10^{-5} cm/s, 7.91 × 10^{-5} cm/s, and 8.87 × 10^{-5} cm/s, respectively. The first path had the largest saturation permeability coefficient, and the 1% →3% path had the smallest.

The analysis shows that during the "first low concentration followed by high concentration" phase, the concentration difference also produced a repulsive force from the outside to the inside of the soil particles, promoting the agglomeration of soil particles,

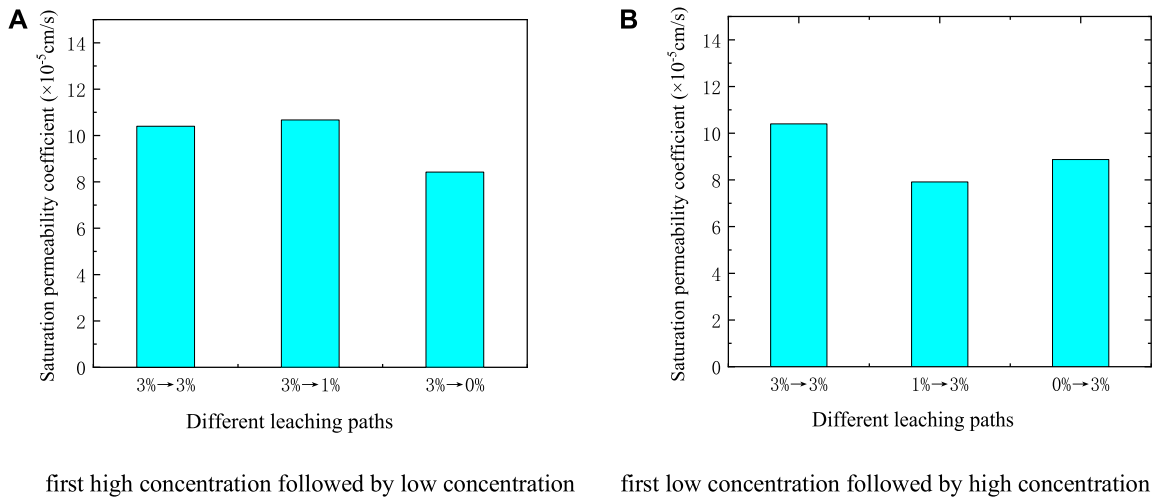

FIGURE 8
The saturated permeability coefficient of different leaching paths **(A)** First high concentration followed by low concentration **(B)** First low concentration followed by high concentration.

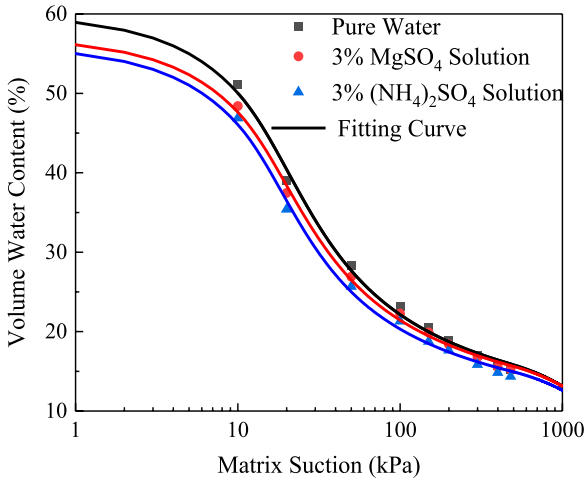

FIGURE 9
Soil-water characteristic curves under different types of leaching solutions.

expanding the seepage channel, and increasing the permeability. When high concentration seepage was used, the ion exchange reaction of rare earths worsened, resulting in the fragmentation and migration of soil particles, and the permeability decreased. Under 1%→3% working conditions, because the effect of the ion exchange reaction was greater than that of the seepage, caused the smallest permeability coefficient by joint action. Under 0%→3% working conditions, the concentration difference caused by the seepage was larger than that under 1%→3% working conditions, and the permeability improved. Therefore, the saturation permeability coefficient under 0%→3% working conditions was larger than that of the former.

4 Soil-water characteristic curves of ionic rare earths under different leaching conditions

4.1 Soil-water characteristic curves under different types of leaching solutions

In order to study the effect of different types of leaching solutions on the soil-water characteristics of ionic rare earths, drying tests were carried out using 3% $(NH_4)_2SO_4$, 3%$MgSO_4$, and pure water, and the water content data were recorded under different matrixes of suction. In this study, the influence of the "hysteresis effect" was not considered, and the drying curve was used to represent the typical soil-water characteristic curve of the ore body. Based on the Fredlund and Xing model, a fitting analysis was carried out, and the obtained soil-water characteristic curves are shown in Figure 9.

The test results show that under pure water conditions, the saturated volume of water content was the largest. Under 3% $(NH_4)_2SO_4$ conditions, the saturated volume water content was the smallest. Under the same matric suction, the water-holding performance of ionic rare earth appeared to be significantly different; pure water had the best water-holding performance, and 3% $(NH_4)_2SO_4$ had the poorest.

Our analysis suggests that pure water did not react with rare earth ions; therefore, the pores of ionic rare earths under pure water conditions basically did not change, resulting in a large, saturated volume of water content. Concentrations of 3% $(NH_4)_2SO_4$ and 3% $MgSO_4$ exchanged with the ionic rare earth, which changed the structure of the soil, resulting in poorer water-holding performance. The capacity of bound water in 3% $(NH_4)_2SO_4$ was stronger than that of 3% $MgSO_4$, but under the same matric suction range, the water content of ionic rare earth under the condition of 3% $(NH_4)_2SO_4$ was lower than that of 3% $MgSO_4$.

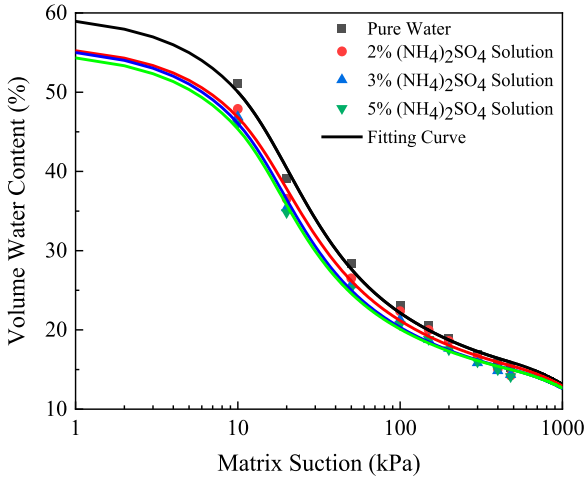

FIGURE 10
Soil-water characteristic curves at different concentrations of leaching solution.

4.2 Soil-water characteristic curves at different concentrations of leaching solution

The soil-water characteristic curves at different concentrations of leaching solutions are shown in Figure 10. It can be seen that the SWCC under pure water conditions was significantly higher than that of other concentrations. Under the same matric suction, the water content of the low concentration leaching solution was slightly higher than that of the high concentration leaching solution. As the concentration of the leaching solution decreased, the volume water content of the ionic rare earth increased, and the water holding capacity also increased.

The analysis suggests that pure water had the greatest water-holding capacity, and that it did not undergo chemical exchange reactions with rare earth ions, which had little effect on the size of ionic rare earth particles. Under other concentrations of leaching conditions, ion exchange reactions occurred, resulting in changes in the internal structure of the soil and changes in water holding capacity. As the concentration of the leaching solution increased, the chemical reaction that occurred during the leaching process became more intense, and the pore structure changed greatly, resulting in the deterioration of the water-holding performance of the ore body at high concentrations.

4.3 Soil-water characteristic curves under different leaching paths

The SWCCs of ionic rare earth under different leaching paths are shown in Figure 11. It can be seen that for 0% →3% working conditions, the water-holding characteristic of an ionic rare earth ore body was the best. Under the same matric suction, its water content was greater than that of other working conditions. For 3%→0% working conditions, ionic rare earth samples had the worst water-holding characteristics. When the matric suction was small, the water content was minimal compared to other working conditions. It can be seen that their water-holding performance was poor, but their residual water content was large. For different path conditions composed of 3% $(NH_4)_2SO_4$ and 1% $(NH_4)_2SO_4$, there was little difference between the two.

The analysis indicates that under "0%→3%" working conditions, because the free water diffused from the high concentration solution to the low concentration solution, this concentration difference produced diffusion force, promoted the formation of agglomerates of fine particles in ionic rare earth samples, and expanded the pores, resulting in a large, saturated volume water content. Under "3%→0%" working conditions, the

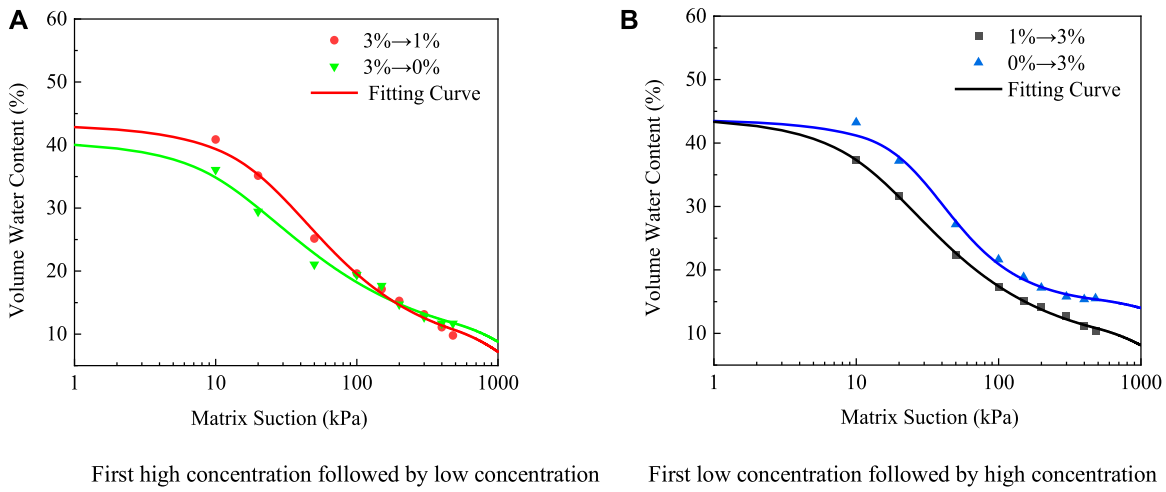

FIGURE 11
Soil-water characteristic curves under different leaching paths **(A)** First high concentration followed by low concentration **(B)** First low concentration followed by high concentration.

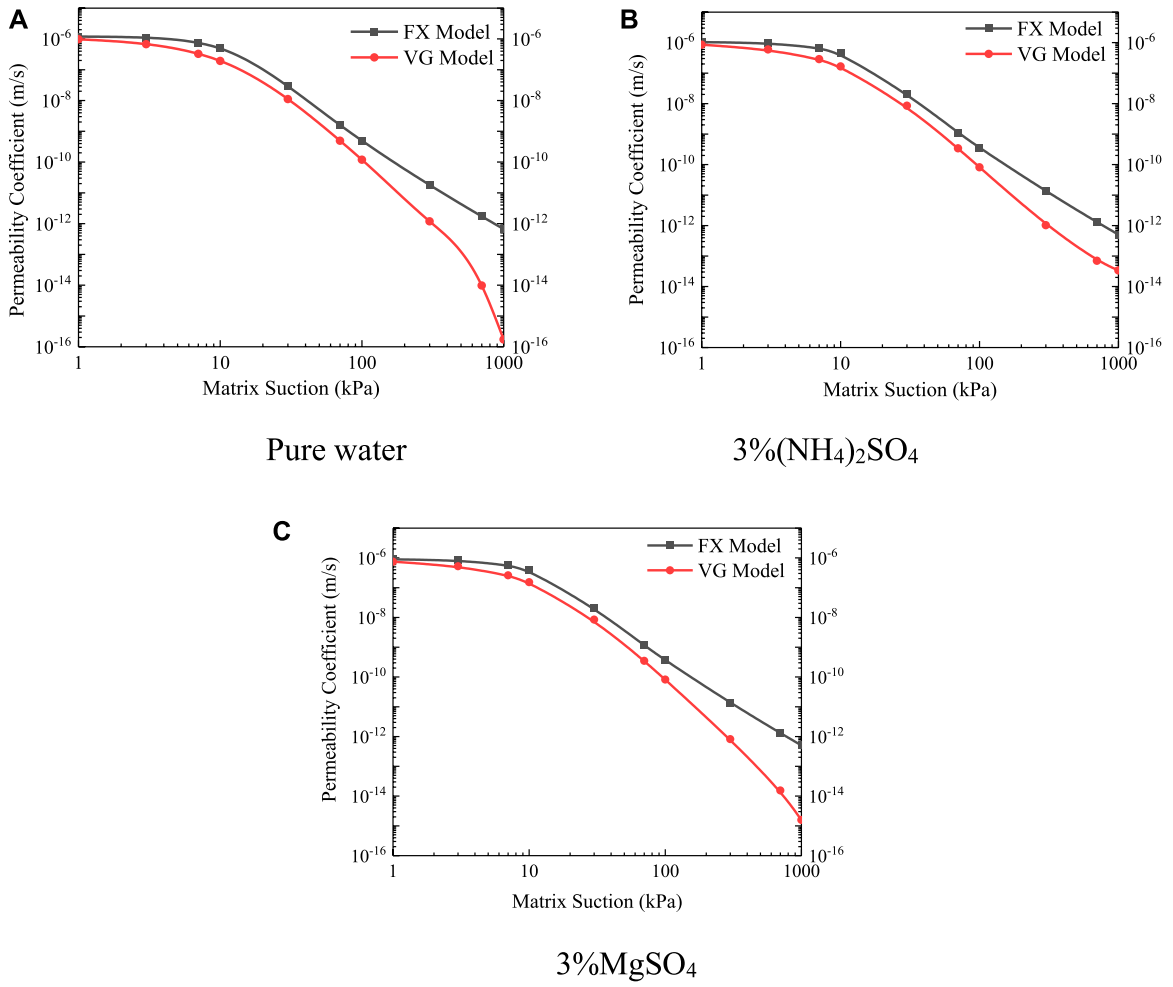

FIGURE 12
Unsaturated permeability curves under different types of leaching solutions **(A)** Pure water **(B)** 3% $(NH_4)_2SO_4$ **(C)** 3% MgSO4.

high concentration of leaching solution disintegrated and transported the ore body particles, resulting in the blockage of pores in the soil and the narrowing of the voids, therefore minimizing the saturated volume water content. For 3%→1% and 1%→3% working conditions, because of the small concentration difference, the diffusion force brought by the concentration difference was smaller than the effect of the ion exchange reaction, its internal structure changed marginally, and so did the water-holding performance of the ore body under these two working conditions.

5 Unsaturated seepage law of ionic rare earths under different leaching conditions

5.1 Unsaturated permeability coefficient function

Unsaturated permeation parameters are difficult to obtain directly from experiments and were calculated indirectly (Zhai et al., 2019). In this study, the Van Genuchten-Mualem model and the Fredlund unsaturated permeability coefficient function were used to calculate the unsaturated permeability function of ionic rare earths, and the unsaturated permeability coefficient was characterized by the saturated permeability coefficient and matric suction.

The Van Genuchten-Mualem model used the Van Genuchten soil-water characteristic curve model and the Mualem permeability equation to obtain the unsaturated permeability coefficient k_u under different matrixes of suction, and is expressed as follows:

$$k_u = k_s \frac{\left\{1 - (a\psi)^{n-1}\left[1 + (a\psi)^n\right]^{-m}\right\}^2}{\left[1 + (a\psi)^n\right]^{m/2}} \quad (4)$$

where k_s is the permeability coefficient in the saturated state; ψ is the matrix suction; a, m, and n are all fitting parameters, where m=1−1/n.

The Fredlund unsaturated permeability function model was obtained by combining the Fredlund and Xing model formula with the Child and Collis-George statistical pore size distribution model, and its expression is as follows:

10.3389/feart.2023.1212017

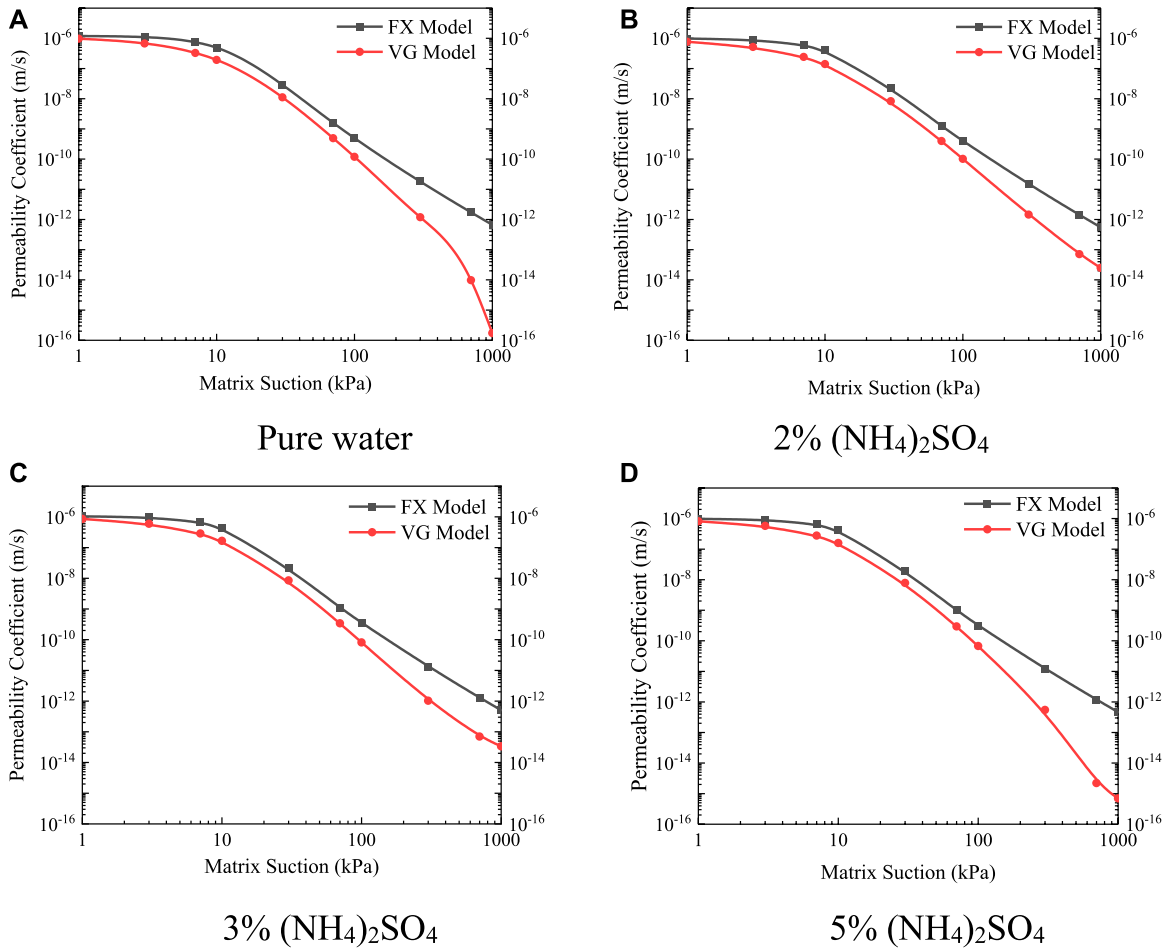

FIGURE 13
Unsaturated permeability curves at different leaching solution concentrations **(A)** Pure water **(B)** 2% (NH4)2SO4 **(C)** 3% (NH4)2SO4 **(D)** 5% (NH4)2SO4.

$$k_u = k_s \frac{\int_{\ln(\psi)}^{b} (\theta(e^y) - \theta(\psi)/e^y)\theta'(e^y)dy}{\int_{\ln(\psi_{aev})}^{b} (\theta(e^y) - \theta_s/e^y)\theta'(e^y)dy} \quad (5)$$

where k_s is the permeability coefficient in the saturated state, ψ is the matrix suction, y is the imaginary variable of the integral $\ln(\psi)$, b generally takes $\ln(10^6)$; ψ_{aev} is the air-entry pressure value, and θ' is the derivative of ψ.

5.2 Unsaturated permeation characteristics under different types of leaching solutions

This study describes the unsaturated permeability characteristics based on the unsaturated permeability coefficient function. The function curves of the unsaturated permeability coefficient under different types of leaching solutions are shown in Figure 12.

The influence of different types of leaching solutions on the unsaturated permeability function of ionic rare earth ores was analyzed, and there was a high correlation between the unsaturated permeability function and the saturated permeability coefficient. In the saturated state, the saturated permeability coefficient of pure water was the largest, followed by 3% $(NH_4)_2SO_4$, and the smallest was 3% $MgSO_4$. In the unsaturated state, the same relationship existed for the unsaturated permeability coefficient of different types of leaching solutions.

In the unsaturated state, the corresponding unsaturated permeability coefficient was the largest in the case of pure water. The types of water in soil are roughly divided into capillary water, membrane water, and gaseous water. By correcting the capillary water model and the valve model of unsaturated soil, it can be seen that the infiltration of capillary water in unsaturated soil was proportional to the effective area of the seepage pore size (31). Combined with the results of saturated permeability characteristics and water-holding properties, it is believed that the main reason is that pure water did not undergo an ion exchange reaction with ionic rare earth ores during the saturated-unsaturated seepage process, and its corresponding effective pore size was the largest and the permeability characteristics are the best. Under the same matric suction, the unsaturated permeability coefficient functions of 3% $(NH_4)_2SO_4$ and 3% $MgSO_4$ were smaller than those of pure water because the exchange reaction between cations and rare earth ions,

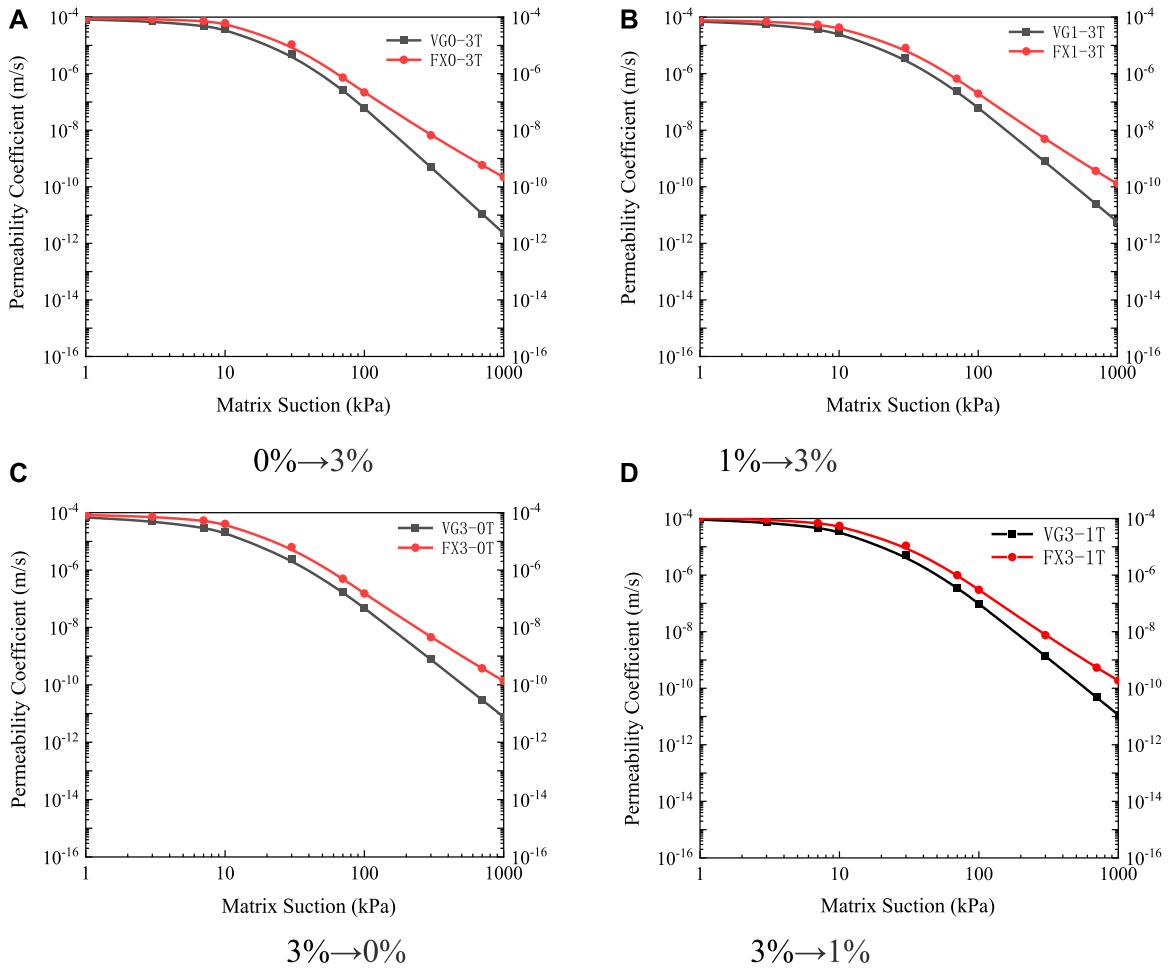

FIGURE 14
Unsaturated permeability curves under different leaching paths **(A)** 0%→3% **(B)** 1%→3% **(C)** 3%→0% **(D)** 3%→1%.

the effective area of the internal pore size of the soil become smaller, and the unsaturated permeability characteristics also become weaker.

5.3 Unsaturated permeation characteristics at different leaching solution concentrations

The unsaturated permeability curves at different leaching solution concentrations are shown in Figure 13. The analysis shows that when the matric suction was small, the unsaturated permeability coefficient function was mainly influenced by the saturated permeability coefficient; the unsaturated permeability coefficient of pure water was the largest, the unsaturated permeability coefficient was consistent with the saturated permeability coefficient, and the unsaturated permeability coefficient of 2% $(NH_4)_2SO_4$ and 5% $(NH_4)_2SO_4$ was smaller than that of 3% $(NH_4)_2SO_4$. With the increase in matric suction, the unsaturated permeability coefficient of different concentrations also changed, and with the increase in concentration, the unsaturated permeability coefficient decreased.

In the case of pure water, the unsaturated permeability coefficient of ionic rare earths was the largest; there was less particle decomposition, less seepage pore blockage, and a larger internal effective pore size. When the matric suction was small, most of the inside of the soil consisted of capillary water, and the unsaturated permeation characteristics of ionic rare earths could be analyzed according to the "valve model." The water inside the soil began to be composed of membrane water; the migration law of water in the water film was significantly different from the migration law of capillary water, and the migration efficiency of the membrane water was closely related to the thickness of the water film on the surface of soil particles. The exchange reaction between NH^{4+} and rare earth ions on the surface of soil particles affected the thickness of membrane water on the surface of soil particles. Under different leaching solution concentrations, with the increase of concentration, the ions exchanged with each other, thereby reducing the thickness of the water film on the surface of soil particles and the permeability characteristic of membrane water in unsaturated soil. The higher the concentration of the leaching solution, the more intense the reaction, the more severe the damage to the water film on the surface of the soil particles, and the lower the unsaturated permeability coefficient.

5.4 Unsaturated permeation characteristics under different leaching paths

The unsaturated permeability curves under different leaching paths are shown in Figure 14. It can be seen that the different leaching paths had an effect on the function of the unsaturated permeability coefficient of ionic rare earths. For the path of "first high concentration followed by low concentration," because of the diffusion force, the internal repulsion of the soil particles was generated from the inside to the outside, which promoted the crushing of the soil particles, blocked the seepage channel, and reduced the unsaturated permeability coefficient. For the path of "first light concentration followed by high concentration," the diffusion force from the outside to the inside was generated inside the soil particles, therefore promoting the condensation of fine soil particles, widening the seepage channel, and increasing the unsaturated permeability coefficient.

The unsaturated permeability characteristics of ionic rare earths were closely related to the seepage channels in the soil. The infiltration of unsaturated soil capillary water was proportional to the effective area of the seepage pore size. Combined with the saturated seepage law and the soil-water characteristic curve, under the leaching path of "0%→3%," the seepage channel was the largest, therefore the unsaturated permeability coefficient was also the largest. Under the leaching path of "3%→0%," its seepage channel was the smallest, therefore the unsaturated permeability coefficient was also the smallest. For the leaching paths of "1%→3%" and "3%→1%," the seepage channel changed marginally, so the difference between the unsaturated permeability coefficient under these two working conditions was small.

6 Conclusion

(1) The type of leaching solution has a certain influence on the permeability characteristics of ionic rare earths, and the saturated permeability coefficients of the ore body are pure water, 3% $(NH_4)_2SO_4$, 3% $MgSO_4$ in descending order under different leaching conditions. When the concentration of the leaching solution increases from 2% to 5%, the saturation permeability coefficient increases and then decreases.

(2) According to the analysis of soil-water characteristic curves, under the conditions of different types of leaching solutions, the water-holding performance of the ore body under pure water conditions was the best, followed by the $MgSO_4$ working conditions, while the $(NH_4)_2SO_4$ working conditions was the worst. As the concentration of the leaching solution increased, the water content of the ore body decreased, and the water-holding capacity also decreased.

(3) The seepage law is related to the leaching path, and the permeability coefficient increased when the concentration was high, followed by a low concentration. When the concentration was first low and then high, the permeability coefficient decreased. Therefore, in the *in situ* leaching process of ionic rare earth ore, the liquid injection method of "high concentration followed by low concentration" can be used to improve the permeability of the soil and further obtain a higher rare earth leaching rate.

(4) Based on the unsaturated permeability function model, the unsaturated permeability coefficient function curve of the ore body under different leaching conditions can be obtained. The unsaturated permeability coefficient predicted by the Fredlund and Xing model is more realistic than the one obtained by the Van Genuchten model. The unsaturated permeability coefficient predicted by the model can provide a more objective and accurate assessment basis for calculating rare earth leaching rates.

Data availability statement

The raw data supporting the conclusion of this article will be made available by the authors, without undue reservation.

Author contributions

Conceptualization, ZG and LL; methodology, ZG; validation, KZ and LL; writing—original draft preparation, ZG and LL; writing—review and editing, ZG, LL, and KZ; supervision, ZG, WZ, and XW; project administration, ZG; funding acquisition, ZG and XW. All authors contributed to the article and approved the submitted version.

Funding

The research was supported by the National Natural Science Foundation of China (Grants Nos. 52004106, 52174113) and the Natural Science Foundation of Jiangxi Province (Grant No. 20224BAB214035).

Conflict of interest

The authors declare that the research was conducted in the absence of any commercial or financial relationships that could be construed as a potential conflict of interest.

Publisher's note

References

Chi, R. A., and Liu, X. M. (2019). Prospect and development of weathered crust elution-deposited rare Earth ore. *J. J. Chin. Soc. Rare Earths* 37 (02), 129–140. doi:10.11785/S1000-4343.20190201

Chiu, C. F., Yan, W. M., and Yuen, Ka-veng. (2012). Estimation of water retention curve of granular soils from particle-size distribution—A bayesian probabilistic approach. *J. Can. Geotechnical J.* 49 (9), 1024–1035. doi:10.1139/t2012-062

Deng, G. Q., and Yang, Y. M. (2016). A Review of the mining technologies of ion-absorbed rare Earth mineral. *J. Chin. Rare Earths.* 37 (03), 129–133. doi:10.16533/J.cnki.15-1099/tf.201603023

Fredlund, D. G., and Pham, H. Q. (2006). "A volume-mass constitutive model for unsaturated soils in terms of two independent stress state variables," in Proceedings of the A. Fourth International Conference on Unsaturated Soils, Lisbon, Portugal, June 2006.

Fredlund, D. G., and Xing, A. (1994). *Erratum*: Equations for the soil-water characteristic curve. *J. Can. geotechnical J.* 31 (4), 1026–1532. doi:10.1139/t94-120

Gao, L. X., Luan, M. T., Yang, Q., and Wang, D. L. (2008). Experimental study of permeability of unsaturated remoulded clays. *J. Rock Soil Mech.* 2008 (08), 2267–2270+2276. doi:10.16285/j.rsm.2008.08.050

Guo, Z. Q., Jin, J. F., Qin, Y. H., Wang, X. J., Zhong, W., and Zhao, K. (2017). Experimental research on one-dimensional horizontal infiltration rules of ion-adsorption rare Earth. *J. Nonferrous Metals Sci. Eng.* 8 (02), 102–106. doi:10.13264/j.cnki.ysjskx.2017.02.017

Guo, Z. Q., Lai, Y. M., Jin, J. F., Zhou, J. R., Zhao, K., and Sun, Z. (2020). Effect of particle size and grain composition on two-dimensional infiltration process of weathered crust elution-deposited rare Earth ores. *J. Trans. Nonferrous Metals Soc. China.* 30 (6), 1647–1661. doi:10.1016/S1003-6326(20)65327-4

Guo, Z. Q., Zhou, J. R., Zhou, K. F., Jin, J. F., Wang, X. J., and Zhao, K. (2021). Soil–water characteristics of weathered crust elution-deposited rare Earth ores. *J. Trans. Nonferrous Metals Soc. China* 31 (05), 1452–1464. doi:10.1016/S1003-6326(21)65589-9

He, Z. Y., Zhang, Z. Y., Chi, R. N., Xu, Z. G., Yu, J. X., Wu, M., et al. (2017). Leaching hydrodynamics of weathered elution-deposited rare Earth ore with ammonium salts solution. *J. J. Rare Earths* 35 (8), 824–830. doi:10.1016/s1002-0721(17)60982-7

Ilankoon, I. M. S. K., Tang, Y., Ghorbani, Y., Northey, S., Yellishetty, M., Deng, X. Y., et al. (2018). The current state and future directions of percolation leaching in the Chinese mining industry: Challenges and opportunities. *J. Mineng.* 125, 206–222. doi:10.1016/j.mineng.2018.06.006

Jin, J. F., Tao, W., Qiu, C., and Guo, Z. Q. (2015). Experimental research on one-dimensional vertical infiltration rule of ionic rare Earth and the effects of maximum particle size. *J. Nonferrous Metals Sci. Eng.* 6 (06), 125–131. doi:10.13264/j.cnki.ysjskx.2015.06.023

Liu, C. F., Zhou, F., Wu, X. Y., Feng, J., and Chi, R. A. (2021). Development and prospect in seepage and mass transfer process of weathered crust elution-deposited rare Earth ore. *J. Chin. Rare Earths.* 42 (01), 111–121. doi:10.16533/j.cnki.15-1099/tf.20210044

Long, P., Wang, G. S., Tian, J., Hu, S. L., and Luo, S. H. (2019). Simulation of one-dimensional column leaching of weathered crust elution-deposited rare Earth ore. *J. Trans. Nonferrous Metals Soc. China* 29 (3), 625–633. doi:10.1016/S1003-6326(19)64972-1

Ma, T. T., Wei, C. F., Xia, X. L., and Chen, P. (2016). Constitutive model of unsaturated soils considering the effect of intergranular physicochemical forces. *J. J. Eng. Mech.* 142(11). doi:10.1061/(asce)em.1943-7889.0001146

Nie, W. R., Zhang, R., He, Z. Y., Zhou, J., Wu, M., Xu, Z. G., et al. (2020). Research progress on leaching technology and theory of weathered crust elution-deposited rare Earth ore. *J. Hydromet.* 193, 105295. doi:10.1016/j.hydromet.2020.105295

Pham, H. Q. (2005). *A volume-mass constitutive model for unsaturated soils.* Saskatoon, Canada: D. The University of Saskatchewan.

Rajkai, K., Sandor, Kabos., Martinus, Th., and Van, Genuchten. (1996). Per-Erik, Jansson. Estimation of water-retention characteristics from the bulk density and particle-size distribution of Swedish soils. *J. Soil Sci.* 161 (12), 832–845. doi:10.1097/00010694-199612000-00003

Van, Genuchten. M. T. (1980). A closed form equation for predicting the hydraulic conductivity of unsaturated soils. *J. Soil Sci. Soc. Am. J.* 44 (5), 892–898. doi:10.2136/sssaj1980.03615995004400050002x

Wang, X. J., Li, Y. X., Huang, G. L., Fang, S. Y., Zhong, W., and Liao, S. Y. (2017). Research of permeability and porosity in ion-type rare Earth leaching process. *J. Chin. Rare Earths.* 38 (5), 47–55. doi:10.16533/j.cnki.15-1099/tf.201705007

Wu, A. X., Yin, S. H., and Li, J. F. (2005). Influential factors of permeability rule of leaching solution in ion-absorbed rare Earth deposits with *in-situ* leaching. *J. J. Central South Univ.* 36 (3), 506–510. doi:10.3969/j.issn.1672-7207.2005.03.031

Yin, S. H., Chen, X., and Jiang, L. C. (2015). Effect of ore particle size on solution capillary seepage in ore heaps. *J. Chin. J. Eng.* 37 (5), 561–567. doi:10.13374/j.issn2095-9389.2015.05.004

Yin, S. H., Qi, Y., Xie, F. F., Chen, X., and Wang, L. M. (2018). Permeability characteristic of weathered crust elution deposited rare Earth ores under different pore structures. *J. Chin. J. Nonferrous Metals.* 28 (5), 1043–1049. doi:10.19476/j.ysxb.1004.0609.2018.05

Zhai, Q., Rahardjo, H., Satyanaga, A., and Dai, G. (2019). Estimation of unsaturated shear strength from soil–water characteristic curve. *J. Acta Geotech.* 14 (6), 1977–1990. doi:10.1007/s11440-019-00785-y

Zhang, Z. Y., He, Z. Y., Yu, J. X., Xu, Z. G., and Chi, R. A. (2016). Novel solution injection technology for *in-situ* leaching of weathered crust elution-deposited rare Earth ores. *J. Hydromet.* 164, 248–256. doi:10.1016/j.hydromet.2016.06.015

Zhou, F., Liu, Q., Feng, J., Su, J. X., Liu, X., and Chi, R. A. (2019). Role of initial moisture content on the leaching process of weathered crust elution-deposited rare Earth ores. *J. Seppur* 217, 24–30. doi:10.1016/j.seppur.2019.02.010